Slow rate of secondary forest carbon accumulation in the Guianas compared with the rest of the Neotropics

Jérôme Chave, Camille Piponiot, Isabelle Maréchaux, Hubert de Foresta, Denis Larpin, Fabian Jörg Fischer, Géraldine Derroire, Grégoire Vincent, Bruno Hérault

HAL Id: mnhn-03989178
https://mnhn.hal.science/mnhn-03989178

Submitted on 28 Apr 2023

Slow rate of secondary forest carbon accumulation in the Guianas compared with the rest of the Neotropics

Jérôme Chave,[1,8] Camille Piponiot,[2] Isabelle Maréchaux,[1,3,4] Hubert de Foresta,[4] Denis Larpin,[5] Fabian Jörg Fischer,[1] Géraldine Derroire,[2] Grégoire Vincent,[4] and Bruno Hérault[6,7]

[1]*Laboratoire Evolution et Diversité Biologique, UMR5174, CNRS–Université Paul Sabatier–IRD, Bâtiment 4R1, 118 route de Narbonne, F-31062 Toulouse Cedex 9, France*
[2]*Cirad, UMR 'Ecologie des Forêts de Guyane' (AgroparisTech, CNRS, Inra, Université des Antilles, Université de la Guyane), F-97379 Kourou Cedex, French Guiana*
[3]*AgroParisTech-ENGREF, 19 Avenue du Maine, F-75015 Paris, France*
[4]*AMAP, Univ Montpellier, IRD, CIRAD, CNRS, INRA, F-34000 Montpellier, France*
[5]*Direction Générale Déléguée aux Musées, Jardins et Zoos, Muséum National d'Histoire Naturelle, 57 rue Cuvier, F-75005 Paris, France*
[6]*Cirad, Univ Montpellier, UR Forests & Societies, F-34000 Montpellier, France*
[7]*INPHB, Institut National Polytechnique Félix Houphouët-Boigny, Yamoussoukro, Ivory Coast*

Abstract. Secondary forests are a prominent component of tropical landscapes, and they constitute a major atmospheric carbon sink. Rates of carbon accumulation are usually inferred from chronosequence studies, but direct estimates of carbon accumulation based on long-term monitoring of stands are rarely reported. Recent compilations on secondary forest carbon accumulation in the Neotropics are heavily biased geographically as they do not include estimates from the Guiana Shield. We analysed the temporal trajectory of aboveground carbon accumulation and floristic composition at one 25-ha secondary forest site in French Guiana. The site was clear-cut in 1976, abandoned thereafter, and one large plot (6.25 ha) has been monitored continuously since. We used Bayesian modeling to assimilate inventory data and simulate the long-term carbon accumulation trajectory. Canopy change was monitored using two aerial lidar surveys conducted in 2009 and 2017. We compared the dynamics of this site with that of a surrounding old-growth forest. Finally, we compared our results with that from secondary forests in Costa Rica, which is one of the rare long-term monitoring programs reaching a duration comparable to our study. Twenty years after abandonment, aboveground carbon stock was 64.2 (95% credibility interval 46.4, 89.0) Mg C/ha, and this stock increased to 101.3 (78.7, 128.5) Mg C/ha 20 yr later. The time to accumulate one-half of the mean aboveground carbon stored in the nearby old-growth forest (185.6 [155.9, 200.2] Mg C/ha) was estimated at 35.0 [20.9, 55.9] yr. During the first 40 yr, the contribution of the long-lived pioneer species *Xylopia nitida*, *Goupia glabra*, and *Laetia procera* to the aboveground carbon stock increased continuously. Secondary forest mean-canopy height measured by lidar increased by 1.14 m in 8 yr, a canopy-height increase consistent with an aboveground carbon accumulation of 7.1 Mg C/ha (or 0.89 Mg C·ha^{-1}·yr^{-1}) during this period. Long-term AGC accumulation rate in Costa Rica was almost twice as fast as at our site in French Guiana. This may reflect higher fertility of Central American forest communities or a better adaptation of the forest tree community to intense and frequent disturbances. This finding may have important consequences for scaling-up carbon uptake estimates to continental scales.

Key words: biomass; carbon; forest; French Guiana; regeneration; secondary forests; tropics.

INTRODUCTION

Tropical forests have undergone massive rates of deforestation and degradation (Hansen et al. 2013) contributing to over 70% of the global terrestrial gross land-use change carbon emissions into the atmosphere (Houghton et al. 2012), which amounts to about 1 Pg C/yr for the period 2006–2015 (Le Quéré et al. 2016). Conversely, tropical emissions have been offset by the regrowth of tropical secondary forests, which have contributed an estimated atmospheric carbon sink of 1.6 Pg C/yr (Pan et al. 2011). Even though estimates remain debated (Liu et al. 2015), regrowing tropical forests have an enormous potential to reduce atmospheric CO_2

concentrations in the next decades (Houghton et al. 2015, Chazdon et al. 2016). Here, we present results from a new long-term study on tropical forest carbon accumulation in French Guiana.

The vast majority of available information on secondary forest succession is based on chronosequence data, where stands of various successional ages are inventoried once, and forest stand properties are plotted against age. In a compilation of chronosequence studies at 43 sites in the Neotropics, Poorter et al. (2016) found an average of 3 Mg C·ha^{-1}·yr^{-1} aboveground carbon (AGC) accumulation rate in the first 20 yr of regrowth, a figure slightly larger than the one assumed in carbon bookkeeping methods (Pan et al. 2011, Houghton et al. 2015). The rate of carbon accumulation varied more than 10-fold across sites, suggesting that there is a large variation in regrowth pathways. This may be explained by the idiosyncrasies of secondary regrowth, by methodological differences across studies, but also possibly by regional differences in environmental conditions.

The forests of the Guianas grow on soils of low fertility owing to the ancient and nutrient-poor Precambrian geological substrate (Quesada et al. 2012), and old-growth forests in this region store more carbon per unit area than the rest of Amazonia (Saatchi et al. 2011). We would therefore expect that the time needed to reach mature forest biomass would be longer in the Guianas than elsewhere in the Neotropics. Few studies on forest secondary succession are, however, available in the Guiana Shield, even though the region covers one-third of Amazonia and is thus highly relevant to continental-scale modeling of tropical forest regeneration (Norden et al. 2015).

Another factor mediating differences in forest recovery rates across the Neotropics may be differences in regional species pools (Norden et al. 2009). Through ecological succession, pioneer species, with fast growth rates, high mortality rates, and low wood density, are progressively superseded by shade-tolerant species able to establish in the forest understory, with high wood density, low growth rates and low mortality rates. (Gómez-Pompa and Vázquez-Yanes 1981). In this classic view of forest succession, shifts in wood density are crucial to determine the carbon accumulation dynamics of a stand (Poorter et al. 2019). Since secondary forests are dominated by a reduced taxon set, it is possible, and desirable, to document how the common tree species contribute to the carbon accumulation dynamics.

Although a great part of our knowledge on forest succession has been derived from chronosequence studies, these present several limitations that hamper robust data interpretation. The key assumption of chronosequence studies is that space can be substituted for time (Johnson and Miyanishi 2008). A pitfall of this approach is the difficulty to trace back past land uses and initial conditions of the sites, which can influence successional trajectories (Martin et al. 2013, Chazdon 2014, Arroyo-Rodríguez et al. 2017). Large sample sizes are needed to

accurately predict the regrowth trajectory in a given forest landscape, since there is a large variation in the explanatory power of fallow age for carbon accumulation inference (Mora et al. 2015, Becknell et al. 2018a). A preferable alternative relies on the long-term monitoring of permanent forest plots, but such studies are currently rare, and seldom extend beyond two decades of monitoring (Feldpausch et al. 2007, Rozendaal and Chazdon 2015).

Another limitation of chronosequence studies is that they are based on a sample of small forest plots (typically ranging from 0.01 to 1 ha; Poorter et al. 2016, Becknell et al. 2018a), which prevents a robust assessment of regeneration dynamics at the landscape scale (Estes et al. 2018). Remote sensing technology offers the opportunity to scale up plot-based carbon accumulation estimates across entire landscapes. Of the remote-sensing methods, aerial laser scanning offers great potential to monitor the successional status of forests (Mascaro et al. 2012, Englhart et al. 2013, Meyer et al. 2013, Ene et al. 2016, Becknell et al. 2018b). ALS provides rapid access to forest structure variables, such as canopy height and structure, both of which vary rapidly as forest succession advances (Peña-Claros 2003, Mora et al. 2015, Rozendaal and Chazdon 2015). Mascaro et al. (2012) used aerial lidar to infer the carbon accumulation of a forest landscape in Panama and, more recently, Becknell et al. (2018b) published similar results for a Brazilian Atlantic landscape of Southern Bahia. However, lidar methods for carbon monitoring are calibrated using contemporaneous forest plots at different successional stages, so this calibration is also predicated on the validity of the chronosequence approach. Aerial lidar has seldom been used to detect changes in canopy height and in canopy structure through time, primarily because the technology has emerged only recently in tropical forest monitoring.

The present study builds on a long-term ecological project at a 25-ha secondary forest stand located within an old-growth forest matrix in French Guiana. This stand was experimentally clear-cut in 1976, and it has been repeatedly monitored thereafter with no human intervention over the past forty years. It thus provides a rare example of a secondary forest, in the Guiana Shield and across the tropics, that has been monitored continuously for decades. We document the carbon accumulation dynamics during the first forty years of secondary succession, both for the whole stand and for the dominant tree taxa.

Based on forest inventories, we first modeled the carbon accumulation trajectory. We hypothesized that carbon accumulation rates would be lower at our site than the mean values reported for the Neotropics (Poorter et al. 2016). Second, we explored the contribution of common species to carbon accumulation and changes in community-mean wood density through time in the stand. Third, we used two aerial lidar surveys to compare the structure of the forest in 2009 and 2017. We hypothesized that forest height would increase through

ecological succession, but also that canopy structure would change. We finally compared our results with those obtained at a wet forest site in Costa Rica using the data published by Rozendaal and Chazdon (2015). To our knowledge, this study is the only other published case of a long-term monitoring of secondary forests in the Neotropics, and for this reason it is the only other study directly comparable to ours.

METHODS

Study site and sampling

The study site is located 15 km southwest of the village of Sinnamary, French Guiana (5.30° N, 53.05° W; Fig. 1). It receives around 3,000 mm/yr mean annual precipitation and has a 2-month dry season (months with <100 mm rainfall) in September and October. The area is covered by moist tropical forest, with a lidar-derived top canopy height exceeding 40 m (Réjou-Méchain et al. 2015). These forests have relatively infertile soils (Grau et al. 2017), tall canopy, and high biomass per area (Saatchi et al. 2011).

In July–August 1976, a 10-ha area was logged over as part of a pulp production project that was abandoned soon thereafter. Not all the stems were removed from the site, and an average of 74 stems/ha were left onsite (stems with lower timber value, such as Chrysobalanaceae). In

August–September 1976, all remaining trees were cut down and the felled area was extended to 500 × 500 m (25 ha). Logs were only partly removed and the logging remains (crowns and roots) were left onsite. About 10% of the soil surface was extensively disturbed by logging activities during the time of operation, and about 15% of the clearing was severely burned by an accidental fire in October 1976 (Sarrailh 1980, 1989, Maury-Lechon 1982, Sarrailh et al. 1990; Fig. 1).

Starting in 1989, a 6.25-ha (250 × 250 m) plot was monitored for all stems ≥10 cm dbh. Stems were mapped, tagged, and their stem diameter measured using a standard protocol. Tree-by-tree reinventory of the plot was conducted every year from 1989 to 1992 and from 1994 to 1996, and approximately every 2 yr from 2003 to 2014. Botanical identifications were initially based on vernacular names, but starting in 2007 a detailed botanical census was conducted. Several of the unidentified trees had died before they could be identified, still resulting in an overall identification rate of over 80% for all the trees dead or alive in the database. In the census conducted in 2014, 87% of the trees were identified. Some genera were common at the onset of the forest regrowth process, and we explored their long-term contribution to the carbon accumulation process. These included the following 11 genera: *Cecropia* (Urticaceae), *Vismia* (Hypericaceae), *Xylopia* (Annonaceae), *Goupia* (Goupiaceae), *Laetia* (Salicaceae), *Tachigali*, *Albizia*,
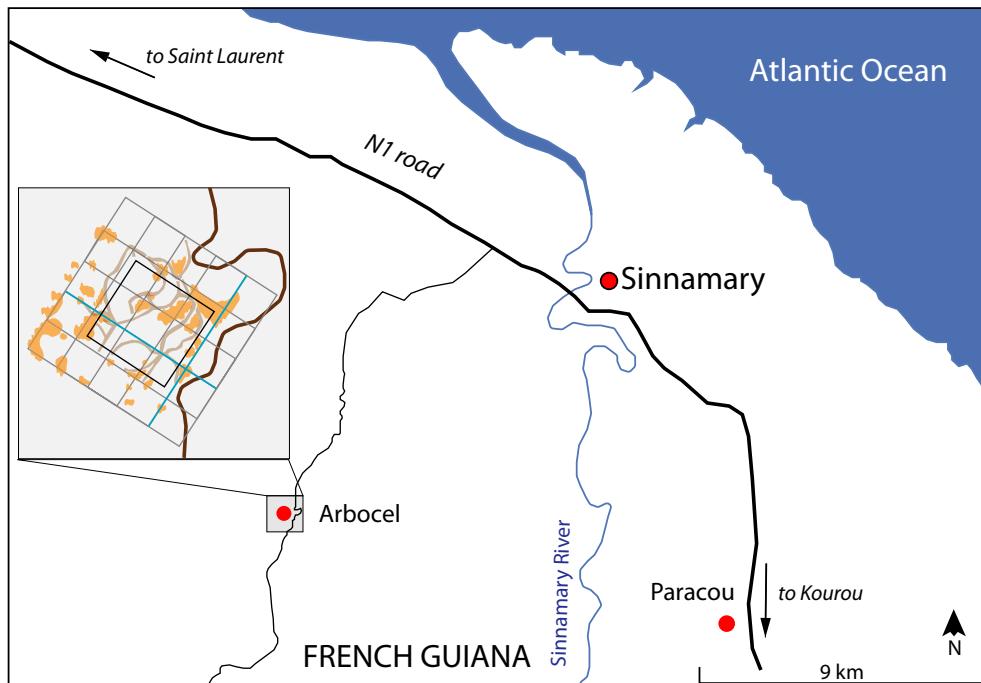

FIG. 1. Map of the study area. Arbocel site is close to the village of Sinnamary, French Guiana. The access to road was unpaved until 2005 (route de Saint Elie). The Paracou Research Station is also illustrated on this map. Inset: map of the 500 × 500 m clear-cut experiment, with access road (in brown), 6.25-ha tree plot (black square), and sapling transects (blue segments). In addition, skid-trail roads are shown in gray, and area burned in 1976 is given in orange (redrawn from Maury-Lechon 1982).

and *Inga* (Fabaceae), *Miconia* (Melastomataceae), *Jacaranda* (Bignoniaceae), and *Byrsonima* (Malpighiaceae). This set of species was selected so as to encompass at least 80% of the carbon stock at the beginning of the sampling in 1989. Through time, more species were added to the inventory, so this proportion declines, but in 2014, the 11 genera still accounted for 66% of the aboveground biomass stock.

Early secondary forests regrowing from a clear-cut site have almost no stems ≥10 cm dbh, and most of the aboveground biomass is held within stems <10 cm dbh. Fortunately, saplings were also sampled early on within the same clear-cut area, but with a slightly different sampling strategy. Three and a half years after land conversion (1980), de Foresta (1983, 1984) sampled two transects of 460 × 2 m (transect 1), and of 532 × 2 m (transect 2). All stems ≥ 1 cm dbh were measured, mapped, and identified to species. In the first half of 1988, Larpin (1989) recensused part of transect 1 (404 × 2 m), again recording all stems ≥1 cm dbh. In 2005, transect 1 was extended to an area of 425 × 4 m, and transect 2 to an area of 530 × 4 m. Finally, in 2016, we inventoried all stems ≥1 cm dbh in nine 0.01-ha square quadrats, evenly located across the permanent tree plot.

As a basis for the carbon accumulation model, we computed stand-level metrics of the ecological succession, including tree density (trees per ha), basal area (BA, the cumulative cross-sectional area of trunks, in m^2/ha), and live aboveground carbon (AGC; carbon mass, in Mg C/ha) for each of the censuses described above. To estimate AGC, we used the allometric model developed in Chave et al. (2014), and propagated wood density, trunk measurement and allometric uncertainties on every live tree of the census to the plot-level estimates using the *biomass* R package (Réjou-Méchain et al. 2017). Wood density estimates were inferred from species-mean values as reported in the global wood density database (Chave et al. 2009), or assigning the plot average wood density to unidentified stems (<20%). AGC was obtained by converting aboveground oven-dry live biomass into AGC assuming 48% of carbon in oven-dry live mass (Martin and Thomas 2011).

We used stem-by-stem inventory data from the transects and 0.01 ha quadrats for stems <10 cm dbh (1980, 1988, 2005 and 2016), and from the 6.25-ha plot for stems ≥10 cm dbh (from 1989 to 2015) in model inference. In addition, we included published aggregated stand basal area records: Prévost (1983) documented the forest regrowth dynamics in two 100 × 10 m plots 3–9 yr after stand abandonment, recording all stems ≥1 cm dbh from which stand basal area was computed (Sarrailh et al. 1990). In 1995, 52 10 × 10 m plots (0.52 ha) were inventoried for all trees ≥1 cm dbh, and the basal area was reported (Toriola Lafuente 1997). All inventories are summarized in Metadata S1.

Carbon accumulation inference

Stems ≥10 cm dbh and stems <10 cm dbh are expected to represent different proportions in biomass and floristic composition through secondary forest succession. Given that they were sampled using different designs, at different times, and with different sampling intensities, we used a statistical model to infer the stand-scale carbon accumulation dynamics, and its uncertainty, during forest recovery. To this end, we chose a Monte Carlo inference scheme under a Bayesian framework. Since basal area was available more frequently than AGC, we first modeled basal area increase through time. From this model, we then inferred the temporal trajectory of AGC and propagated uncertainties from the data sources to our results.

Mean basal area accumulation through time was modeled in the two compartments as follows:

$$\widehat{BA_{sapling}}(t) = \theta_1 \times \left(1 - \exp(-\theta_{2a}t)\right) + \theta_3 \times \exp\left(-[\ln(t/\theta_4)/\theta_5]^2\right) \quad (1)$$

$$\widehat{BA_{tree}}(t) = \theta_6 \times (1 - \exp(-\theta_{2b}t)). \quad (2)$$

In Eq. 1, the first term describes the accumulation of sapling basal area through time, θ_1 being the asymptotic sapling basal area, and θ_{2a} the rate at which this asymptote is reached. The second term of Eq. 1 represents "boom-and-bust" dynamics, with θ_3 the maximum excess sapling basal area, θ_4 (in yr) the time at which this maximum is reached, and θ_5 a kurtosis parameter. Eq. 2 models the tree basal area accumulation, where θ_6 is the asymptotic tree basal area, and the rate at which the asymptote is reached, θ_2, differs in the two compartments, hence the subscripts *a* and *b*. Aboveground carbon was linked to basal area through a power-law function:

$$\widehat{AGC_{sapling}} = \exp(\theta_9) \times \left(BA_{sapling}\right)^{\theta_{10}} \times \left[\widehat{AGC_{tree}}\right]^{\theta_{11}} \quad (3)$$

$$\widehat{AGC_{tree}} = \exp(\theta_7) \times (BA_{tree})^{\theta_8}. \quad (4)$$

In Eq. 3, the term in $\widehat{AGC_{tree}}$ models a coupling between the sapling and the tree stages effect, since sapling density is expected to correlate with large tree density through a self-thinning effect. Inference of the model parameters was performed using a Hamiltonian Monte-Carlo algorithm (see Appendix S1). The maximal (asymptotic) value of $\widehat{AGC} = \widehat{AGC_{sapling}} + \widehat{AGC_{tree}}$, AGC_{max}, was inferred from the model in Eqs. 3 and 4 using as a prior a normal distribution with mean 185 Mg C/ha and a standard deviation of 12 Mg C/ha,

which reflects the mean and variability among observed values in mature forest plots of the Paracou permanent monitoring system, located some 15 km east of our study site (Fig. 1), and covered by a similar vegetation (Blanc et al. 2009).

Carbon balance in trees

Next, we explored how AGC dynamics in the tree compartment ≥10 cm dbh were affected by AGC accumulation through recruits and tree growth, and AGC loss due to stem mortality. We expected that AGC ingrowth exceeded loss. We conducted this analysis from 1989 to 2014. Carbon balance can be measured using the following equation:

$$\Delta \text{AGC}_t = \text{NPP}_{w,t} + \text{Recruit}_t - \text{Loss}_t \qquad (5)$$

where ΔAGC is the change in AGC, NPP_w is the carbon uptake due to woody growth, Recruit is the carbon uptake due to tree recruitment (individual trees crossing the dbh threshold of 10 cm), and Loss is the carbon loss due to tree mortality. We emphasize here that this NPP_w refers to the allocation to aboveground woody growth of trees >10 cm dbh and not to the entire ecosystem NPP (see Malhi [2012] for a discussion). These terms are defined by

$$\text{NPP}_{w,t} = \sum_i \frac{\text{AGC}_{i,t+1} - \text{AGC}_{i,t}}{\Delta t},$$
$$\text{Recruit}_t = \sum_{i'} \frac{\text{AGC}_{i',t+1}}{\Delta t}, \ \text{Loss}_t = \sum_{i''} \frac{\text{AGC}_{i'',t}}{\Delta t} \qquad (6)$$

where the first summation runs over all trees alive in both censuses, the second summation runs over saplings at census t that had become trees at census $t + 1$, and the third summation runs over trees that died between the censuses. Some of the consecutive inventories displayed large variation in mortality, and the reported stand fluxes were smoothed using a moving average of the form $\bar{x}_i = 0.25x_{i-1} + 0.5x_i + 0.25x_{i+1}$.

Aerial laser scanning of the study site

We conducted two overflights of the study site using small-footprint aerial lidar sensors. Our first campaign was conducted in April 2009 with a Riegl LMS-280i (*RIEGL* Laser Measurement Systems GmbH, Horn, Austria) single return storage capacity operating in last return mode. The second campaign was conducted in September 2017 with a Riegl LMSQ560 full waveform with multiple-return storage capacity. The area overlapping the two surveys was of 400 ha. The lidar point cloud was analysed by first extracting the ground points, to generate a digital terrain model at 1-m spatial resolution.

We next extracted top-of-canopy points to generate a canopy height model also at 1-m spatial resolution. The 500 × 500 m regrowing forest had a road cutting through the east part of the plot, and we masked this

area with a 10-m buffer. Since the two surveys used different sensors and point densities, which could bias the estimated changes in canopy structure between the two surveys, we determined a reference region of the same size as the regrowth plot taken at random in the undisturbed forest a few hundred meters away. We compared the canopy height changes between the two surveys in the 25-ha regrowth plot and in the nearby old-growth forest control plot.

We finally compared normalized vegetation profiles between these two plots computed using the 2017 survey. Normalization uses the ray tracing of laser shots in a three-dimensional mesh to compute local transmittance, which is then inverted to estimate local vegetation density (Tymen et al. 2017, Vincent et al. 2017). This procedure resulted in the estimation of the area of scatterers (both leaves and woody components) within each 1-m³ voxel of the canopy. This index is called the plant area density (PAD) and is measured in m² of scatterers per unit volume (m²/m³). We averaged this PAD for each 1-m canopy height layer and compared these PAD profiles computed for 25 50 × 50 m subplots in the secondary forest plot and an equivalent number in the old-growth forest plot. Finally, we summed the PAD vertically, to compute the plant area index (PAI), which is the cumulative area of scatterers per area of ground (in m²/m²). This PAI is similar to the commonly measured leaf area index, but also includes woody components.

Comparison of AGC recovery with other Neotropical secondary forest sites

Finally, we used carbon accumulation at 20 yr reported by Poorter et al. (2016) for comparison. We selected 13 lowland Amazonian sites, that receive at least 1,500 mm rainfall annually, have a weak seasonality, as characterized by a climatic water deficit ≥400 mm/yr (Aragão et al. 2007), and are located <400 m in elevation: three were in Bolivia (El Tigre, El Turi, Bolpebra), seven in Brazil (three in Eastern Para, two around Manaus, and two around the Rio Madeira), two in Colombia (Araracuara and near San Carlos de Rio Negro), and one in Peru (Pucallpa).

Zwetsloot (1981) described a further site in Suriname (Blakawatra) where a 120 × 80 m experimental plot was set up in 1967 after clear cutting an old-growth forest on well-drained sandy soil to sticky loam soil. Basal area increased to 15.2 m²/ha within the first 11 yr of abandonment (Zwetsloot 1981: Fig. 8). However, it was not possible to infer carbon accumulation based on basal area increment and we excluded this study from the comparison.

We also took advantage of the recent publication by Rozendaal and Chazdon (2015) who reported on a long-term monitoring in six 1-ha secondary forest plots in Costa Rica. We used their census data to recalculate tree AGC at the three plots that were totally clear-cut prior to abandonment using the same AGC inference methods

as for the French Guiana plot. Specifically, we included in the comparison Juan Enriquez (JE, Chilamate), Lindero Sur (LSUR, La Selva), and Lindero El Peje (LEP, La Selva). To facilitate comparison between the French Guiana and Costa Rica sites, we constructed a simpler AGC accumulation model, as follows:

$$\widehat{AGC} = \widehat{AGC_{sampling}} + \widehat{AGC_{tree}}$$
$$= \theta_{12} + (AGC_{max} - \theta_{12}) \times (1 - \exp(-\theta_{13}t)). \quad (7)$$

This model is such that, as time t tends to infinity, the expectation on AGC tends to AGC_{max}. We fit Eq. 7 separately on the three Costa Rica data sets, using a slightly lower prior on AGC_{max} (normal prior, mean = 170 Mg C/ha, standard deviation = 12 Mg C/ha; based on old-growth sites in Rozendaal and Chazdon 2015). For French Guiana, we also assumed a normal prior for AGC_{max} but with different values (mean = 185 Mg C/ha, standard deviation = 12 Mg C/ha) as above.

RESULTS

Using the model in Eqs. 1–4, we found that AGC stocks rose quickly from 0 to 37.8 (95% credibility interval 21.7, 60.1) Mg C/ha within the first 10 yr, the time at which the transient boom-and-bust dynamics of saplings reached its maximum (Fig. 2). Saplings contributed 61% of the AGC stock 10 yr after stand abandonment. Twenty years after stand abandonment, AGC stock was 64.2 (46.4, 89.0) Mg C/ha, and saplings contributed 33.8% of the stocks. After 40 yr of regrowth, total AGC stock was estimated at 101.3 (78.7, 128.5) Mg C/ha, and sapling AGC at 13.4 (3.7, 26.3) Mg C/ha. The maximal AGC, AGC_{max}, was inferred at 185.6 (155.9, 200.2) Mg C/ha. Using the simplified exponential model (Eq. 7), we inferred the time needed to accumulate one-half of the maximal AGC at 35.0 (20.9, 55.9) yr.

Aerial laser scanning revealed that after 40 yr (in 2017), median canopy height was 19.5 m in the regrowing plot, compared with 28.7 m in the old-growth forest control site. Comparing the 2017 survey to the 2009 survey ($\Delta t = 8$ yr), we found that the regrowing forest gained 1.14 m more in mean canopy height than the control plot, and top-canopy height (95% percentile across 1-m^2 subplots) gained 1.99 m (Table 1). Thus, ALS-derived mean canopy height increment was in average 0.14 m/yr and top-canopy height increment was 0.25 m/yr. The standard deviation in canopy height growth rates across 1-m^2 subplots was smaller in the regrowing plot (3.1 m) than in the control plot (5.8 m). The secondary forest plot had a significantly lower plant area index (PAI, 10.4 vs. 13.8 m^2/m^2). However, the plant area density (PAD) peaked at higher levels in the secondary forest, suggesting that the top canopy is denser in the secondary forest than in the old-growth forest (Fig. 3).
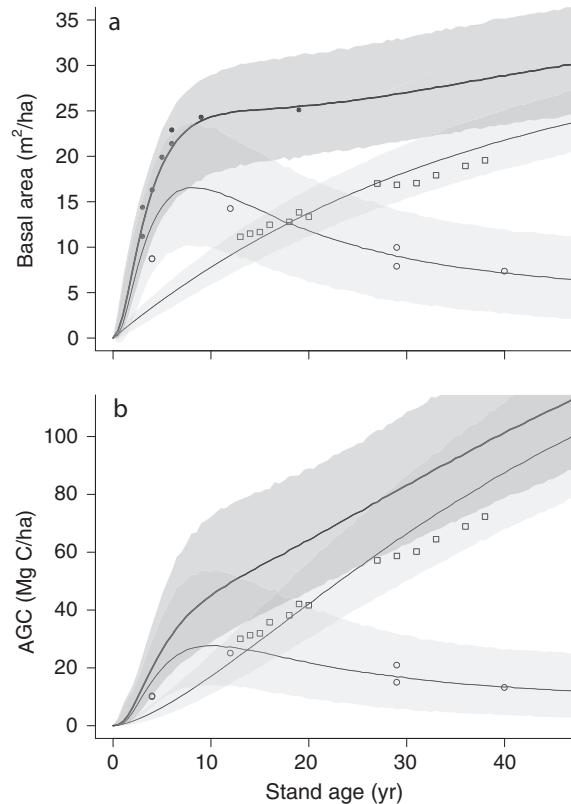

FIG. 2. Changes in forest structure during a 40-yr secondary regrowth in a forest of French Guiana: (a) basal area and (b) aboveground carbon (AGC). In both panels, open circles represent sapling measurements (<10 cm dbh), open squares represent tree measurements (≥10 dbh cm), and solid circles represent total measurements (saplings plus trees). Lines represent the best fits of Eqs. 1–4, with light-shaded areas showing the 95% credibility intervals of the sapling and tree models. Dark-shaded areas represent the 95% credibility intervals of the curves for saplings plus trees.

TABLE 1. Canopy height in the regrowing plot compared to the control plot in 2009 and in 2017.

Parameter	Regrowing plot			Control plot			Δ–ΔC
	2009	2017	Δ	2009	2017	ΔC	
Mean (m)	17.81	19.42	1.61	27.53	28	0.47	1.14
Median (m)	18.04	19.43	1.39	28.27	28.56	0.29	1.10
90% (m)	23.01	24.86	1.85	36.00	36.06	0.06	1.79
95% (m)	24.43	26.48	2.05	38.00	38.06	0.06	1.99

Notes: Canopy height was measured from the canopy height model at 1-m resolution using four possible metrics: mean, median, top 90%, and top 95%. Canopy height increase was named Δ in the regrowing plot and Δ_C in the control plot.

Changes in AGC through time were quantified for 11 taxa (Fig. 4a). *Cecropia* spp. declined in dominance in the first 20 yr, followed by *Vismia* spp., while *Xylopia nitida* Dunal, *Laetia procera* (Poepp.) Eichler, and
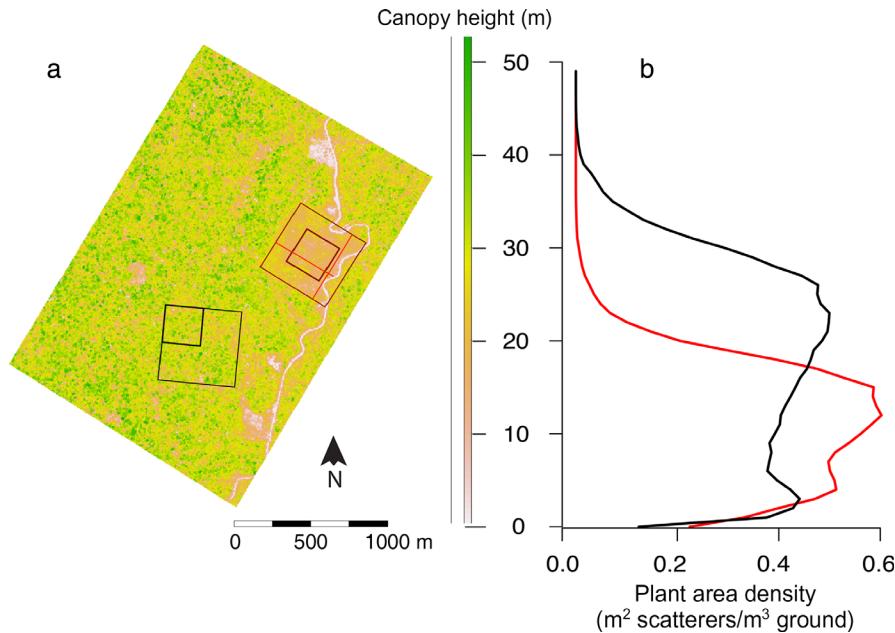
Fig. 3. Remote sensing of the study area using a small-footprint aerial lidar scanning technique (in 2017). (a) Canopy height model at 1-m resolution, where the secondary forest site is clearly visible at the Northeast of the scene (a small fraction of the stand is crossed by a paved road). (b) Plant area density (area of scatterers per unit volume) as inferred from a ray-tracing algorithm (see *Methods*). In both panels, the regrowing forest plot is illustrated in red, and the control plot in black. Panel a and b have the same y axis.

Goupia glabra Aubl. increased in dominance throughout the study period.

Community-wide properties of the forest stand changed significantly during the first 40 yr of regrowth. Basal-area weighted wood density across trees ≥10 cm dbh increased from 0.48 g/cm^3 12 yr after stand abandonment to 0.60 g/cm^3 after 38 yr (Fig. 4b), still far from the old-growth estimate of 0.68 g/cm^3 in these forests (Chave et al. 2008).

After 15 yr of regrowth, woody NPP in trees ≥10 cm dbh varied between 1.7 and 2.2 Mg C·ha^{-1}·yr^{-1} depending on years (Fig. 5), except for a spike at 2.5 Mg C·ha^{-1}·yr^{-1}. Carbon accumulation due to recruitment was fairly stable throughout the survey period, around 0.5–1 Mg C·ha^{-1}·yr^{-1}. Stem mortality was variable across years, with a spike of mortality 14 yr after stand abandonment, largely explaining the interannual variation in net carbon accumulation (which varied from 1.2 to over 2.5 Mg C·ha^{-1}·yr^{-1}).

We also compared our results with those obtained elsewhere in the Neotropics. Across the 13 sites retained from Poorter et al. (2016), AGC values 20 yr after abandonment ranged between 40.6 Mg C/ha and 107.8 Mg C/ha, with a mean of 74.7 ± 17.9 Mg C/ha (mean ± SE across sites). Thus, our value of 64.2 Mg C/ha after 20 yr is in the lower end, though not exceptionally low, of the range reported for Amazonian rainforests.

Finally, fitting Eq. 7 at the three Costa Rica plots, we found that maximal AGC was 176 (152, 184) Mg C/ha at Juan Enriquez, 157 (147, 177) Mg C/ha at Lindero El Peje, and 162 (150, 182) Mg C/ha at Lindero Sur

(Fig. 6). Given these inferred estimates, the time to reach one-half of the maximum AGC was almost twice as short as at our site, at 24 (21, 28.5) yr at Juan Enriquez, 16 (14, 19) yr at Lindero El Peje, and 20 (17.5, 23.5) yr at Lindero Sur.

DISCUSSION

Long-term trends in carbon accumulation at a French Guiana site

We here report results on the long-term aboveground carbon accumulation dynamics in a secondary forest of French Guiana. Initially, AGC accumulation peaked 3 yr after abandonment. AGC accumulation rate remained high after 10 yr and declined slowly thereafter. For instance, between 32 and 40 yr after abandonment, the inferred AGC accumulation rate was 1.73 Mg C·ha^{-1}·yr^{-1} on average, almost one-half of the mean of the first 20 yr (3.2 Mg C·ha^{-1}·yr^{-1}). Thus, the potential of secondary forests for rapid carbon accumulation decreases beyond the 20-yr horizon of forest regrowth, and this slowdown should be accounted for in carbon mitigation plans.

After 10 yr, sapling AGC stock declined, while tree AGC continued to increase, a consequence of increasing size-biased competition in regrowing mixed-species forests (Farrior et al. 2016). However, after 40 yr of regrowth, sapling AGC still represented 13.2% of total AGC, a proportion that was twice larger than our estimate after 100 yr of regrowth. By comparison, sapling
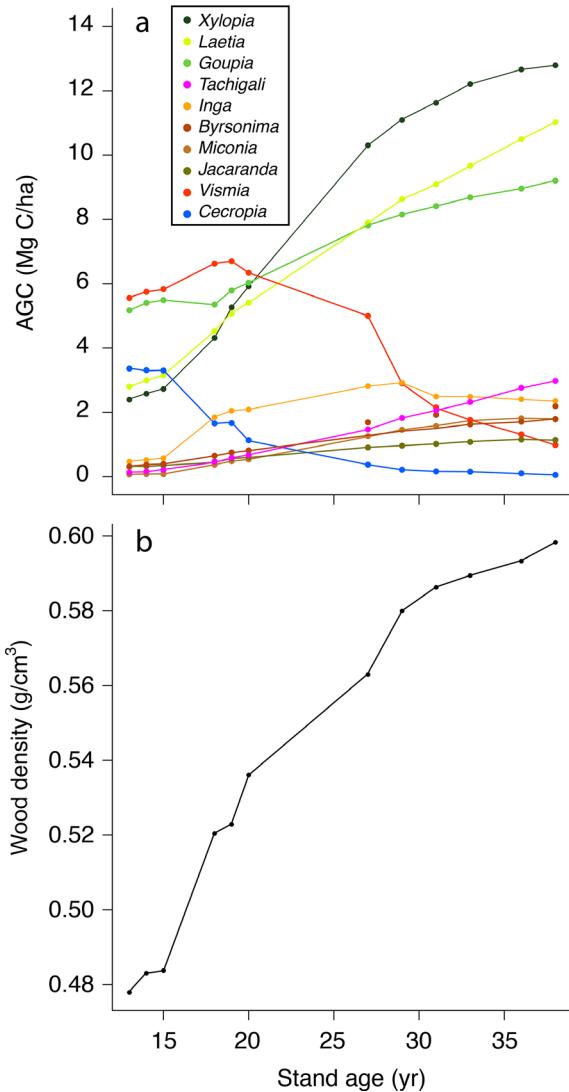
FIG. 4. Community-wide changes in trees (≥10 dbh cm). (a) Changes in aboveground carbon (AGC) for 10 of the 11 dominant tree genera of trees in the permanent inventory plot (*Albizia* was hidden by the curves of *Byrsonima* and *Miconia* and was therefore omitted). (b) Changes in stand-averaged wood density (weighted by basal area; values are means). The tree census started 12 yr after plot abandonment.

AGC was estimated at 4 Mg C/ha in a nearby old-growth forest, i.e., about 2% of the total stock (Baraloto et al. 2011). Therefore, this study confirms that the decline in sapling AGC stock is slow and that saplings remain a significant component of the carbon stock during a long period during forest regrowth. Similar to our study, Hughes et al. (1999) found that sapling AGC was over twice as large in 50-yr-old secondary forests as in nearby primary forests of Los Tuxtlas, Mexico (see their Table 4). Thus, stems <10 cm dbh account for a significant part of the biomass dynamics in secondary forests. Ignoring them would therefore result in a serious underestimation of the aboveground carbon stock.
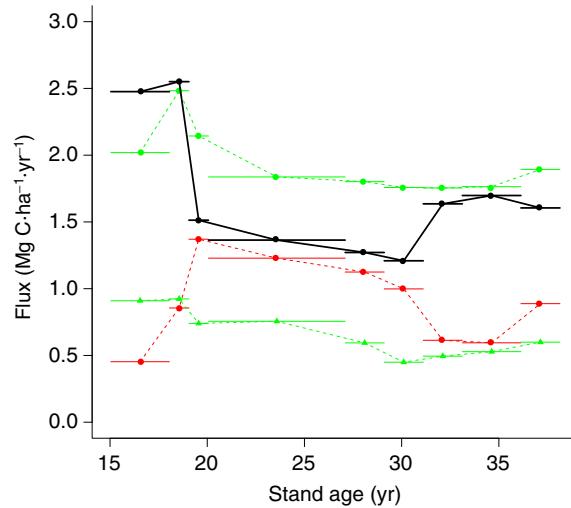

FIG. 5. Carbon fluxes in the tree plot. Fluxes were measured between two consecutive inventories, and the time span between these inventories is represented by horizontal lines. Green circles represent aboveground woody NPP in trees ≥10 cm dbh (NPP$_w$, in Eqs. 5 and 6), green triangles represent ingrowth into the ≥10 cm dbh tree category (Recruit), and red circles represent carbon loss due to mortality (Loss). Black circles with solid black lines represent the balance of these components (woody NPP plus ingrowth minus loss).
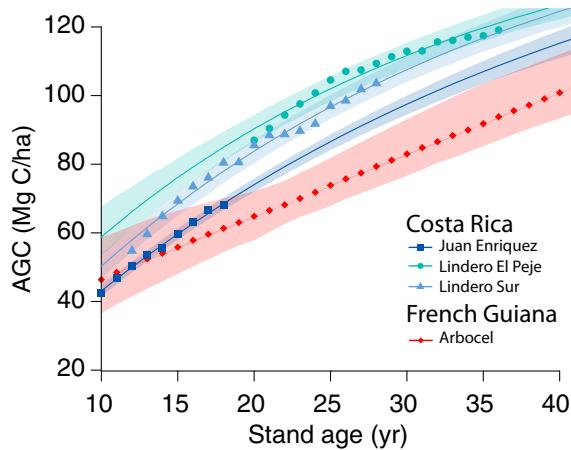

FIG. 6. Comparison of the AGC accumulation curve in French Guiana (red diamonds and solid lines) and that of three sites in Costa Rica (shades of blue; circles, triangles, and squares; data from Rozendaal and Chazdon 2015). Lines and 95% credibility intervals were obtained from fitting the model of Eq. 7.

Our study site represents a special case compared with studies conducted at other Neotropical sites. We studied a single large plot (6.25 ha) monitored through time. This is unlike many other sites, where the chronosequence approach was used to approximate the regrowth of tropical forests (Poorter et al. 2016). Regular monitoring has been limited to a small number of Neotropical secondary forest sites that form the backbone of the

NeoSelvas project (NeoSelvas 2012). Of these, the majority of the inventory plots have a sampling area < 0.1 ha (Chiapas, Mexico; Manaus, Brazil), and only the 1-ha Costa Rica plots are of a size comparable to our study (cf. the comparison in the present study).

Monitoring of large plots requires more labor and is therefore more logistically challenging, but it produces a much more robust signal in floristic and forest structure metrics. There is, however, a trade-off with environmental coverage. Since we provide results at a single site only, we may overlook the variability due to environmental conditions within the Guiana Shield, and our study may not be representative of carbon recovery rates within the whole ecoregion. While we acknowledge this limitation, the present work advances our knowledge on the carbon recovery potential of Neotropical secondary forests, when compared with other studies of the region.

Remote sensing and carbon accumulation monitoring

Remote sensing technology is able to detect variation in forest carbon stocks from variation in forest canopy height and this is an opportunity for carbon mapping (Mascaro et al. 2012). For instance, the space GEDI mission by NASA will use full waveform lidar to infer forest canopy structure and height in forests worldwide (Dubayah et al. 2010, Saatchi et al. 2012, Qi and Dubayah 2016). Another mission, BIOMASS (P-band Synthetic Aperture Radar, SAR) funded by the European Space Agency, will give similar information but over a 5-yr period. Importantly, these approaches are calibrated using forest plots of different AGC stocks and thus substitute space for time as in the chronosequence approach.

In our study, canopy height, as measured by lidar, changed distinctively in 8 yr of succession (2009–2017). Comparing canopy-height metrics in 2009 and 2017 revealed that the canopy height increment was larger for the 95% top-canopy height metric (+1.99 m during the period) than for mean-canopy height (+1.14 m). The faster increase of top-canopy height than mean-canopy height is explained by significant changes in canopy structure. The 41-yr secondary forest was still very different from the neighboring old-growth forest, being much shorter and with a plant area density more densely packed toward the top of the canopy (Fig. 3b). However, the plant area index (PAI) was lower in the secondary forest than in the neighboring old-growth forest. Thus, even if the canopy of secondary forests is more densely packed toward the top, the lower PAI of the secondary forest stand implies that ground retrieval is not an issue in secondary forest stands, because the laser beam transmission through the canopy directly depends on PAI, according to the Beer-Lambert law. Ecologically, the fact that secondary forest trees first tend to pack the top canopy before lower canopy strata is consistent with expectations, but this also implies that, on a per-leaf basis, the photosynthetic activity of a secondary forest should be higher than that of an old-growth forest.

In the space-for-time approach, information from the literature can be used to predict the rate of carbon accumulation in the forest. For instance, using aerial lidar data and forest inventories from French Guiana and Gabon, Labrière et al. (2018) showed that AGC was related to mean canopy height linearly and consistently across continents, with a slope of 6.2 Mg C·ha^{-1}·m^{-1}. Using this model, our mean canopy height increment of 1.14 m during the study period predicts a carbon accumulation of +7.1 Mg C/ha. Because we have a direct measurement of carbon accumulation at this site, we can use it to assess this estimate provided by a generic model. In 2009, the total forest AGC was estimated at 57.1 Mg C/ha, and in 2017 at 64.2 Mg C/ha, thus taking the difference of the values, we obtain +7.1 Mg C/ha, which is precisely the model estimate.

We conclude that at our site, both the space-for-time substitution and the simple assumption that AGC increases linearly with mean-canopy height yield consistent predictions. It would be important to further examine how forest structure varies along other successional pathways, and at other sites to further expand the potential of remote-sensing technology in secondary forest monitoring and carbon mitigation support.

Influence of floristic turnover on carbon accumulation

The boom and bust dynamics we described in the early stages of forest regrowth was primarily driven by a drastic floristic turnover, as has been documented elsewhere in the tropics (Gómez-Pompa and Vázquez-Yanes 1981, Peña-Claros 2003). After 10 yr, short-lived pioneers at our site, e.g., *Vismia* spp., and *Cecropia obtusa* were almost fully replaced by a cohort of species referred to as long-lived pioneers (Finegan 1996, Rüger et al. 2018). The most typical long-live pioneer taxa, *Xylopia nitida*, *Goupia glabra*, and *Laetia procera*, are present early on during the successional process, but they are also frequently found as emergents in primary forests. At our site, they were still increasing in dominance after 40 yr, which may result from their remarkable physiology that enables them to thrive in the high evaporative demand conditions of both early successional stages and high canopy position. For example, photosynthetic uptake of *Goupia glabra* appears to be maintained during the dry season (Silva et al. 2011), owing to its relatively low leaf water potential at turgor loss point (Maréchaux et al. 2016). The patterns of change in dominance of *Vismia* were intermediate between short-lived and long-lived pioneers. This pattern may be linked to the partial burning of the site, because *Vismia* grows well on land that has been cleared by burning (Norden et al. 2011), and is also consistent with the light-demanding physiology of this genus (Silva et al. 2011).

The long-term tree inventory within our study plot allowed us to explore the interannual patterns of aboveground woody NPP and carbon loss in trees. This analysis confirmed that the plot acts as a significant carbon

sink throughout the monitoring period, but also evidenced strong patterns of temporal variation (Fig. 5). For instance, carbon loss through mortality varied two-fold with a peak at almost 1.5 Mg C·ha^{-1}·yr^{-1} after 20 yr of regeneration, followed by a low at around 0.6 Mg C·ha^{-1}·yr^{-1} after year 30. These patterns could be partly due to the small sample size of tree mortality events between any two censuses, but are also, at least in part, due to the species turnover at the site, especially the rapid decline in species with low wood density, such as *Vismia* and *Cecropia*, which were replaced by species with intermediate wood density during the same period. Importantly, we assumed that wood density was constant among trees within a species. While this assumption appears reasonable at the community scale, evidence suggests that at least some species shift in wood density along succession (Plourde et al. 2015). If verified, that would imply that more research is necessary to clarify the demographic drivers of the carbon cycle in secondary forests (Muscarella et al. 2017).

Regional variation in carbon accumulation

Across the Neotropics, regrowing forests have different disturbance histories, soil fertility, proximities to seed sources, climate conditions, and all these factors may alter the successional trajectory of the forest (Chazdon 2003, Chazdon et al. 2007, Arroyo-Rodríguez et al. 2017). Our study site is a special case as it gathers favorable conditions for enhanced recovery: it was abandoned directly after clear-cut, part of the biomass was left onsite, and it is surrounded by old-growth forest. While we should therefore have expected a relatively rapid recovery, we found that recovery rates were relatively slow compared to other rainforest sites. Even though methodological differences across studies may contribute to the observed variability, we hypothesize that the slow recovery is due to the floristic composition and the relatively poor soils in the Guiana Shield.

To our knowledge, the only study on secondary forest carbon accumulation in the Guiana Shield previous to ours was that of Saldarriaga et al. (1988), near the town of San Carlos de Rio Negro (the chronosequence plots were established on both sides of the Venezuela–Colombia border). AGC accumulation was exceptionally low, at 40.6 Mg C/ha after 20 yr of regeneration, much lower than at our site (64 Mg C/ha). This slow pace of carbon accumulation could be explained by fertility constraints as these forests grow on extremely nutrient-poor soils (Jordan 1982). In contrast, our site can be seen as a best-case scenario for carbon accumulation: the soil is clay rich, the secondary forest site is surrounded by mature vegetation. Also, the site has been immediately abandoned after the first clear-cut operation, and is not embedded within a profoundly transformed landscapes, or submitted to repeated pressures, as many other Neotropical secondary forests (Arroyo-Rodríguez et al. 2017). Our study demonstrates that even in this favorable condition, carbon accumulation is slower than in the rest of the lowland Amazon (74.7 Mg C/ha after 20 yr, range 40.6–107.8; $n = 13$; Poorter et al. 2016), due to a combination of low soil fertility (Quesada et al. 2012) and high AGC stocks (Saatchi et al. 2011). Consistent with this finding, a modeling study has recently confirmed that soil properties explain a significant fraction of the variation in carbon accumulation across Neotropical secondary forests (Medvigy et al. 2019).

Cole et al. (2014), studying changes in floristic composition from pollen cores at many tropical sites, found that Central American forests tended to recover from disturbances twice as fast as South American forests. We found that regrowth dynamics were about twice as fast in sites in Costa Rica than at our site, confirming the argument of Cole et al. (2014). This finding is of relevance to the mapping of the carbon sequestration potential in secondary Neotropical forests, as done by Chazdon et al. (2016). The carbon accumulation curve used by Chazdon et al. (2016) is of the Michaelis-Menten form, $\mathrm{AGC} = \mathrm{AGC}_{\max} \times \mathrm{Age}/(a_{50} + \mathrm{Age})$, where a_{50} is the time to reach one-half of the maximum stock of carbon. They modeled a_{50} as a function of bioclimatic variables and found that the rate of carbon accumulation varied little and was primarily controlled by climate. We proposed a slightly modified formulation to fit the same data, in the form of Eq. 7, which can be rewritten as $\widehat{\mathrm{AGC}} = \mathrm{AGC}_0 + \left(\mathrm{AGC}_{\max} - \mathrm{AGC}_0\right) \times \left(1 - \exp\left(-\mathrm{Age}/\bar{a}\right)\right)$, where AGC_0 is the initial aboveground carbon stock and $\bar{a}$ is the typical recovery time. When $\mathrm{AGC}_0 = 0$, the two models give remarkably similar fits of the data, but when $\mathrm{AGC}_0 \neq 0$, Eq. 7 provides a better fit to the data (Appendix S1: Table S1). It would be interesting to reassess this question of the best functional form to model secondary forest carbon accumulation.

An interpretation of the difference in the recovery from disturbances between our site in French Guiana and the sites in Costa Rica (Fig. 6) is that many Central American forests grow on fertile soil derived from volcanic substrates and should recover faster than in French Guiana. Also, these forests have long been exposed to major disturbances, such as hurricanes or volcanoes, and their flora may recover faster from disturbances. Focusing on differences in the physiological ecology of pioneer species between Costa Rica and French Guiana could help unravel whether the fast recovery of these forests is related to an adaptation to disturbance, or to higher soil fertility.

Conclusions

We found that, at our site in French Guiana, the carbon accumulation rate was at the low end of chronosequence data for Latin America and for Amazonia. This could be because the vast forested area underlain by the Guiana Shield displays a low carbon accumulation potential. Also, the first 20 yr of carbon accumulation dynamics are a poor predictor of the next 20 yr. This

result is important for carbon mitigation strategies (Chazdon et al. 2016) and confirms that more long-term studies should be documented across the Neotropics. One opportunity to better assimilate field data, remote sensing information, and ecological hypotheses into predictive frameworks is offered by individual-based forest growth models (Shugart et al. 2015, Maréchaux and Chave 2017, Rödig et al. 2017). We hope that carefully documented studies such as the one provided here will accelerate the development and intercomparison of such models.

Literature Cited

Aragão, L. E. O., Y. Malhi, R. M. Roman-Cuesta, L. O. Anderson, and Y. E. Shimabukuro. 2007. Spatial patterns and fire response of recent Amazonian droughts. Geophysical Research Letters 34, L07701.

Arroyo-Rodríguez, V., F. P. Melo, M. Martínez-Ramos, F. Bongers, R. L. Chazdon, J. A. Meave, N. Norden, B. A. Santos, I. R. Leal, and M. Tabarelli. 2017. Multiple successional pathways in human-modified tropical landscapes: new insights from forest succession, forest fragmentation and landscape ecology research. Biological Reviews 92:326–340.

Baraloto, C. et al. 2011. Disentangling stand and environmental correlates of aboveground biomass in Amazonian forests. Global Change Biology 17:2677–2688.

Becknell, J. M., S. Porder, S. Hancock, R. L. Chazdon, M. A. Hofton, J. B. Blair, and J. R. Kellner. 2018a. Chronosequence predictions are robust in a Neotropical secondary forest, but plots miss the mark. Global Change Biology 24:933–943.

Becknell, J. M., M. Keller, D. Piotto, M. Longo, M. N. dos Santos, M. A. Scaranello, R. B. de Oliveira Cavalcante, and S. Porder. 2018b. Landscape-scale lidar analysis of aboveground biomass distribution in secondary Brazilian Atlantic forest. Biotropica 50:520–530.

Blanc, L., M. Echard, B. Hérault, D. Bonal, E. Marcon, J. Chave, and C. Baraloto. 2009. Dynamics of aboveground carbon stocks in a selectively logged tropical forest. Ecological Applications 19:1397–1404.

Chave, J., et al. 2014. Improved allometric models to estimate the aboveground biomass of tropical trees. Global Change Biology 20:3177–3190.

Chave, J., J. Olivier, F. Bongers, P. Châtelet, P.-M. Forget, P. van der Meer, and P. Charles-Dominique. 2008. Above-ground biomass and productivity in a rain forest of eastern South America. Journal of Tropical Ecology 24:355–366.

Chave, J., D. Coomes, S. Jansen, S. L. Lewis, N. G. Swenson, and A. E. Zanne. 2009. Towards a worldwide wood economics spectrum. Ecology Letters 12:351–366.

Chazdon, R. L. 2003. Tropical forest recovery: legacies of human impact and natural disturbances. Perspectives in Plant Ecology, Evolution and Systematics 6:51–71.

Chazdon, R. L. 2014. Second growth: the promise of tropical forest regeneration in an age of deforestation. University of Chicago Press, Chicago, Illinois, USA.

Chazdon, R. L., S. G. Letcher, M. van Breugel, M. Martínez-Ramos, F. Bongers, and B. Finegan. 2007. Rates of change in tree communities of secondary Neotropical forests following major disturbances. Philosophical Transactions of the Royal Society B 362:273–289.

Chazdon, R. L. et al. 2016. Carbon sequestration potential of second-growth forest regeneration in the Latin American tropics. Science Advances 2:e1501639.

Cole, L. E. S., S. A. Bhagwat, and K. J. Willis. 2014. Recovery and resilience of tropical forests after disturbance. Nature Communications 5:3096.

de Foresta, H. 1983. Hétérogeneité de la vegetation pionnière en forêt tropicale humide: exemple d'une coupe papetière en forêt guyanaise. Acta Oecologica 4:221–235.

de Foresta, H. 1984. Heterogeneity in early tropical forest regeneration after cutting and burning: Arbocel, French Guiana. Pages 242–253 in A. C. Chadwick and S. L. Sutton, editors. Tropical rain forest, The Leeds Symposium. Leeds Philosophical & Litterary Society, Leeds, UK.

Dubayah, R. O., S. L. Sheldon, D. B. Clark, M. A. Hofton, J. B. Blair, G. C. Hurtt, and R. L. Chazdon. 2010. Estimation of tropical forest height and biomass dynamics using lidar remote sensing at La Selva, Costa Rica. Journal of Geophysical Research: Biogeosciences 115:G00E09.

Ene, L. T. et al. 2016. Large-scale estimation of aboveground biomass in miombo woodlands using airborne laser scanning and national forest inventory data. Remote Sensing of Environment 186:626–636.

Englhart, S., J. Jubanski, and F. Siegert. 2013. Quantifying dynamics in tropical peat swamp forest biomass with multitemporal LiDAR datasets. Remote Sensing 5:2368–2388.

Estes, L., P. R. Elsen, T. Treuer, L. Ahmed, K. Caylor, J. Chang, J. J. Choi, and E. C. Ellis. 2018. The spatial and temporal domains of modern ecology. Nature Ecology & Evolution 2:819.

Farrior, C. E., S. A. Bohlman, S. Hubbell, and S. W. Pacala. 2016. Dominance of the suppressed: Power-law size structure in tropical forests. Science 351:155–157.

Feldpausch, T. R., C. D. C. Prates-Clark, E. Fernandes, and S. J. Riha. 2007. Secondary forest growth deviation from chronosequence predictions in central Amazonia. Global Change Biology 13:967–979.

Finegan, B. 1996. Pattern and process in neotropical secondary rain forests: the first 100 years of succession. Trends in Ecology and Evolution 11:119–124.

Gómez-Pompa, A., and C. Vázquez-Yanes. 1981. Successional studies of a rain forest in Mexico. Pages 246–266 in D. C. West, H. H. Shugart, and D. B. Botkin, editors. Forest succession, concepts and applications. Springer-Verlag, New York, New York, USA.

Grau, O. et al. 2017. Nutrient-cycling mechanisms other than the direct absorption from soil may control forest structure and dynamics in poor Amazonian soils. Scientific Reports 7:45017.

Hansen, M. C. et al. 2013. High-resolution global maps of 21st-century forest cover change. Science 342:850–853.

Houghton, R. A., J. L. House, J. Pongratz, G. R. van der Werf, R. S. DeFries, M. C. Hansen, C. Le Quéré, and N. Ramakutty. 2012. Carbon emissions from land use and land-cover change. Biogeosciences 9:5125–5142.

Houghton, R. A., B. Byers, and A. A. Nassikas. 2015. A role for tropical forests in stabilizing atmospheric CO2. Nature Climate Change 5:1022–1023.

Hughes, R. F., J. B. Kauffman, and V. J. Jaramillo. 1999. Biomass, carbon, and nutrient dynamics of secondary forests in a humid tropical region of Mexico. Ecology 80:1892–1907.

Johnson, E. A., and K. Miyanishi. 2008. Testing the assumptions of chronosequences in succession. Ecology Letters 11:419–431.

Jordan, C. F. 1982. The nutrient balance of an Amazonian rain forest. Ecology 63:647–654.

Labrière, N. et al. 2018. In situ data from the TropiSAR and AfriSAR campaigns as a support to upcoming spaceborne biomass missions. IEEE JSTARS 99:1–11.

Larpin, D. 1989. Floristic composition and structure of a 11.5 year old secondary forest in French Guiana. Revue d'Ecologie (Terre et Vie) 44:209–224.

Le Quéré, C. et al. 2016. Global carbon budget 2016. Earth System Science Data 8:605–649.

Liu, Y. Y., A. I. van Dijk, R. A. De Jeu, J. G. Canadell, M. F. McCabe, J. P. Evans, and G. Wang. 2015. Recent reversal in loss of global terrestrial biomass. Nature Climate Change 5:470–474.

Malhi, Y. 2012. The productivity, metabolism and carbon cycle of tropical forest vegetation: Carbon cycle of tropical forests. Journal of Ecology 100:65–75.

Maréchaux, I., and J. Chave. 2017. An individual-based forest model to jointly simulate carbon and tree diversity in Amazonia: description and applications. Ecological Monographs 87:632–664.

Maréchaux, I., M. K. Bartlett, P. Gaucher, L. Sack, and J. Chave. 2016. Causes of variation in leaf-level drought tolerance within an Amazonian forest. Journal of Plant Hydraulics 3:004.

Martin, A. R., and S. C. Thomas. 2011. A reassessment of carbon content in tropical trees. PLoS ONE 6:e23533.

Martin, P. A., A. C. Newton, and J. M. Bullock. 2013. Carbon pools recover more quickly than plant biodiversity in tropical secondary forests. Proceedings of the Royal Society B 280:20132236.

Mascaro, J., G. P. Asner, D. H. Dent, S. J. DeWalt, and J. S. Denslow. 2012. Scale-dependence of aboveground carbon accumulation in secondary forests of Panama: a test of the intermediate peak hypothesis. Forest Ecology and Management 276:62–70.

Maury-Lechon, G. 1982. Régénération forestière en Guyane française: recrû sur 25 ha de coupe papetière en forêt dense humide (Arbocel). Bois et Forêts des Tropiques 197:3–21.

Medvigy, D., G. Wang, Q. Zhu, W. J. Riley, A. M. Trierweiler, B. G. Waring, X. Xu, and J. S. Powers. 2019. Observed variation in soil properties can drive large variation in modelled forest functioning and composition during tropical forest secondary succession. New Phytologist 223:1820–1833.

Meyer, V., S. S. Saatchi, J. Chave, J. W. Dalling, S. Bohlman, G. A. Fricker, C. Robinson, M. Neumann, and S. Hubbell. 2013. Detecting tropical forest biomass dynamics from repeated airborne lidar measurements. Biogeosciences 10:5421–5438.

Mora, F., M. Martínez-Ramos, G. Ibarra-Manríquez, A. Pérez-Jiménez, J. Trilleras, and P. Balvanera. 2015. Testing chronosequences through dynamic approaches: time and site effects on tropical dry forest succession. Biotropica 47:38–48.

Muscarella, R., M. Lohbeck, M. Martínez-Ramos, L. Poorter, J. E. Rodríguez-Velázquez, M. van Breugel, and F. Bongers. 2017. Demographic drivers of functional composition dynamics. Ecology 98:2743–2750.

NeoSelvas. 2012. http://neoselvas.wordpress.uconn.edu

Norden, N., R. L. Chazdon, A. Chao, Y. H. Jiang, and B. Vílchez-Alvarado. 2009. Resilience of tropical rain forests: tree community reassembly in secondary forests. Ecology Letters 12:385–394.

Norden, N., R. C. Mesquita, T. V. Bentos, R. L. Chazdon, and G. B. Williamson. 2011. Contrasting community compensatory trends in alternative successional pathways in central Amazonia. Oikos 120:143–151.

Norden, N. et al. 2015. Successional dynamics in Neotropical forests are as uncertain as they are predictable. Proceedings of the National Academy of Sciences USA 112:8013–8018.

Pan, Y. et al. 2011. A large and persistent carbon sink in the world's forests. Science 333:988–993.

Peña-Claros, M. 2003. Changes in forest structure and species composition during secondary forest succession in the Bolivian Amazon. Biotropica 35:450–461.

Plourde, B. T., V. K. Boukili, and R. L. Chazdon. 2015. Radial changes in wood specific gravity of tropical trees: inter-and intraspecific variation during secondary succession. Functional Ecology 29:111–120.

Poorter, L. et al. 2016. Biomass resilience of Neotropical secondary forests. Nature 530:211–214.

Poorter, L. et al. 2019. Wet and dry tropical forests show opposite successional pathways in wood density but converge over time. Nature Ecology & Evolution 3:928–934.

Prévost, M.-F. 1983. Etude de la régénération: la végétation secondaire, piste de Saint-Elie en Guyane. Pages 195–213 in J. M. Sarrailh, editor. Le Projet ECEREX (Guyane): analyse de l'écosystème forestier tropical humide et des modifications apportées par l'homme. ORSTOM report, ORSTOM Editions, Paris.

Qi, W., and R. O. Dubayah. 2016. Combining Tandem-X InSAR and simulated GEDI lidar observations for forest structure mapping. Remote Sensing of Environment 187:253–266.

Quesada, C. A. et al. 2012. Basin-wide variations in Amazon forest structure and function are mediated by both soils and climate. Biogeosciences 9:2203–2246.

Réjou-Méchain, M., B. Tymen, L. Blanc, S. Fauset, T. R. Feldpausch, A. Monteagudo, O. L. Phillips, H. Richard, and J. Chave. 2015. Using repeated small-footprint LiDAR acquisitions to infer spatial and temporal variations of a high-biomass Neotropical forest. Remote Sensing of Environment 169:93–101.

Réjou-Méchain, M., A. Tanguy, C. Piponiot, J. Chave, and B. Hérault. 2017. BIOMASS: an R Package for estimating aboveground biomass and its uncertainty in tropical forests. Methods in Ecology and Evolution 8:1163–1167.

Rödig, E., M. Cuntz, J. Heinke, A. Rammig, and A. Huth. 2017. Spatial heterogeneity of biomass and forest structure of the Amazon rain forest: linking remote sensing, forest modelling and field inventory. Global Ecology and Biogeography 26:1292–1302.

Rozendaal, D., and R. L. Chazdon. 2015. Demographic drivers of tree biomass change during secondary succession in northeastern Costa Rica. Ecological Applications 25:506–516.

Rüger, N., L. S. Comita, R. Condit, D. Purves, B. Rosenbaum, M. D. Visser, S. J. Wright, and C. Wirth. 2018. Beyond the fast–slow continuum: demographic dimensions structuring a tropical tree community. Ecology Letters 21:1075–1084.

Saatchi, S. S. et al. 2011. Benchmark map of forest carbon stocks in tropical regions across three continents. Proceedings of the National Academy of Sciences USA 108:9899–9904.

Saatchi, S., L. Ulander, M. Williams, S. Quegan, T. LeToan, H. Shugart, and J. Chave. 2012. Forest biomass and the science of inventory from space. Nature Climate Change 2:826–827.

Saldarriaga, J. G., D. C. West, M. L. Tharp, and C. Uhl. 1988. Long-term chronosequence of forest succession in the upper

Rio Negro of Colombia and Venezuela. Journal of Ecology 76:938–958.

Sarrailh, J.-M. 1980. L'écosystème forestier guyanais. Etude écologique de son évolution sous l'effet des transformations en vue de sa mise en valeur. Bois et Forêts des Tropiques 189:31–36.

Sarrailh, J.-M. 1989. L'opération ECEREX. Etudes sur la mise en valeur de l'écosystème forestier guyanais après déboisement. Le point sur les recherches en cours. Bois et Forêts des Tropiques 219:79–97.

Sarrailh, J.-M., H. de Foresta, G. Maury-Lechon, and M.-F. Prévost. 1990. La régénération après coupe papetière: Parcelle Arbocel. Pages 187–208 *in* J. M. Sarrailh, editor. Mise en valeur de l'écosystème forestier guyanais. INRA-CTFT, Paris, France.

Shugart, H. H., G. P. Asner, R. Fischer, A. Huth, N. Knapp, T. Le Toan, and J. K. Shuman. 2015. Computer and remote-sensing infrastructure to enhance large-scale testing of individual-based forest models. Frontiers in Ecology and the Environment 13:503–511.

Silva, C. E. M., J. F. C. Gonçalves, and E. C. Alves. 2011. Photosynthetic traits and water use of tree species growing on abandoned pasture in different periods of precipitation in Amazonia. Photosynthetica 49:246–252.

Toriola Lafuente, D. 1997. Régénération naturelle en Guyane Française: ARBOCEL, une jeune forêt secondaire de 19 ans. Unpublished Doctoral Dissertation. Paris University, Paris, France.

Tymen, B., G. Vincent, E. A. Courtois, J. Heurtebize, J. Dauzat, I. Maréchaux, and J. Chave. 2017. Quantifying micro-environmental variation in tropical rainforest understory at landscape scale by combining airborne LiDAR scanning and a sensor network. Annals of Forest Science 74:32.

Vincent, G., C. Antin, M. Laurans, J. Heurtebize, S. Durrieu, C. Lavalley, and J. Dauzat. 2017. Mapping plant area index of tropical evergreen forest by airborne laser scanning. A cross-validation study using LAI2200 optical sensor. Remote Sensing of Environment 198:254–266.

Zwetsloot, H. 1981. Forest succession on a deforested area in Suriname. Turrialba 31:369–379.

Supporting Information

Additional supporting information may be found online at: http://onlinelibrary.wiley.com/doi/10.1002/eap.2004/full